Journal of Alloys and Compounds 676 (2016) 9–14

Contents lists available at ScienceDirect

Journal of Alloys and Compounds

journal homepage: http://www.elsevier.com/locate/jalcom

Low temperature sintering and microwave dielectric properties of $MnZrNb_2O_8$ ceramics with H_3BO_3 addition

J.X. Bi, C.F. Xing, C.H. Yang, H.T. Wu*, X.S. Jiang

School of Materials Science and Engineering, University of Jinan, Jinan 250022, China

ARTICLE INFO

Article history:
Received 1 February 2016
Received in revised form
17 March 2016
Accepted 19 March 2016
Available online 22 March 2016

Keywords:
$MnZrNb_2O_8$
Microwave dielectric properties
Solid-state method
H_3BO_3 addition

ABSTRACT

The effects of H_3BO_3 additions on sintering characteristic, phase composition, microstructure and microwave dielectric properties of $MnZrNb_2O_8$ ceramics were investigated. The $MnZrNb_2O_8$ ceramics were prepared by the solid-state method. The phase composition, microstructure and elemental composition of the ceramics were studied using X-Ray Diffraction, Scanning Electron Microscopy and Energy Dispersive Analysis. Only a single-phase $MnZrNb_2O_8$ was formed in $MnZrNb_2O_8$ ceramics with H_3BO_3 addition. A small amount of H_3BO_3 successfully reduced the sintering temperature of $MnZrNb_2O_8$ ceramics from 1250 to 1200 °C without much degradation of the microwave dielectric properties. In addition, the τ_f values were shifted to positive direction with the increase of H_3BO_3 contents. Typically, the $MnZrNb_2O_8$ ceramic with 1 wt% H_3BO_3 sintered at 1250 °C for 4 h exhibited excellent microwave dielectric properties with $\varepsilon_r = 25.80$, $Q{\cdot}f = 28{,}419$ GHz and $\tau_f = -8.4$ ppm/°C.

1. Introduction

With the development of high frequency wireless communication technology, microwave dielectric ceramics such as duplexers, resonators, antennas and oscillators have attracted much commercial and scientific attention [1–4]. For these applications of high frequency wireless communication, the microwave dielectric materials should have a high dielectric constant, a high quality factor and a near-zero temperature coefficient of resonant frequency, which are desirable for minimization of the microwave circuit component, maximum signal intensity and adaptation to environmental temperature changes [5,6]. Moreover, low sintering temperature is also required to match with low-loss and low-melting point conductors in fabrication of dielectric devices. Some methods are usually used to reduce the sintering temperature, such as adding low-melting glass, chemical synthesis and using starting powders with smaller particle size [7–11]. In general, liquid phase sintering by adding glass or low melting point materials such as B_2O_3, V_2O_5, $BaCu(B_2O_5)$ and $ZnO–B_2O_3–SiO_2$ is known as the effective and inexpensive way to obtain dense sintered ceramics. However, the added glass may react with the matrix, which is detrimental to the microwave dielectric properties. Thus, the component and the amount of glass should be carefully designed. H_3BO_3 is recognized as an excellent additive for its lower melting point (450 °C) and lower cost. Besides, H_3BO_3 can be dissolved in water or alcohols, which would benefit the mixing of glass and matrix. In our previous work, the effects of H_3BO_3 addition on the sintering behavior and microwave dielectric properties of $MgZrNb_2O_8$ were investigated. Due to the incorporation of H_3BO_3, the sintering temperature of the $MgZrNb_2O_8$ ceramics was lowered effectively [11].

Recently, more attentions have been paid to the clinic crystal $MnZrNb_2O_8$ with $P2/c$ space group due to their excellent microwave dielectric properties [12–14]. Murthy et al. [12] firstly reported $MnZrNb_2O_8$ ceramics sintered at 1400 °C exhibited microwave dielectric properties of ε_r=16.7, $Q{\cdot}f$ = 40,700 GHz and $\tau_f = -29.6$ ppm/°C. The crystal cell parameters of $MnZrNb_2O_8$ were a = 4.80327 Å, b = 5.62108 Å, c = 5.08225 Å with the β angle of 91.595°. In our previous work, the microwave dielectric properties of pure phase $MnZrNb_2O_8$ ceramics had been investigated systematically as a function of sintering temperatures. The ceramic sintered at 1250 °C for 4 h had a dielectric constant of 24.62, a $Q{\cdot}f$ value of 27,936 GHz and a temperature coefficient of −52.11 ppm/°C [14]. However, the high sintering temperature limited the applications of the ceramics in microwave devices. In order to reduce the sintering temperature and improve the microwave dielectric properties of $MnZrNb_2O_8$, the H_3BO_3 addition was chosen as sintering aids. Furthermore, the relationships among phase

* Corresponding author.
E-mail address: mse_wuht@ujn.edu.cn (H.T. Wu).

http://dx.doi.org/10.1016/j.jallcom.2016.03.144
0925-8388/

composition, densification, bond valence, H_3BO_3 additions and microwave dielectric properties of $MnZrNb_2O_8$ ceramics were also detailed in the present report.

2. Experimental procedure

High-purity oxide powders (>99.9%) of MnO, ZrO_2 and Nb_2O_5 were used as the starting materials. The powders were mixed with H_3BO_3 (x = 0, 1, 2.5, 5, 7.5 wt%) according to the desired composition of $MnZrNb_2O_8$ and ground in ethanol with ZrO_2 balls for 8 h. All the slurries were dried and calcined at 1050 °C for 4 h. The powders were then mixed with polyvinyl alcohol as a binder, granulated and pressed into cylindrical disks of 10 mm diameter and about 5 mm height at the pressure of 200 MPa. These pellets were preheated at 500 °C for 4 h to expel the binder and then sintered at 1050–1250 °C for 4 h in air at a heating rate of 5 °C/min.

Phase analysis of samples were conducted with the help of a Rigaku diffractometer (Model D/MAX-B, Rigaku Co., Japan) using Ni filtered CuKα radiation (λ = 0.1542 nm) at 40 kV and 40 mA settings. The apparent densities of the sintered pellets were measured using the Archimedes method (Mettler ToledoXS64). A network analyzer (N5234A, Agilent Co., America) was used for the measurement of microwave dielectric properties. Dielectric constants were measured using Hakki-Coleman post-resonator method by exciting the TE011 resonant mode of dielectric resonator by using an electric probe as suggested by Hakki and Coleman [15]. Unloaded quality factors were measured using TE01d mode by the cavity method [16]. All measurements were made at room temperature and in the frequency of 8–12 GHz. The temperature coefficient of the resonant frequency (τ_f) was defined as follows:

$$\tau_f = \frac{f_{85} - f_{25}}{60 \times f_{25}} \times 10^6 \ (ppm/^\circ C) \quad (1)$$

where f_{85} and f_{25} represent the resonant frequencies at 85 °C and 25 °C, respectively.

3. Results and discussion

The X-ray diffraction patterns of the $MnZrNb_2O_8$ ceramics doped with different amounts of H_3BO_3 sintered at 1250 °C for 4 h were shown in Fig. 1. All the diffraction peaks were indexed based on the JCPDS file number 48-0331 for $MnZrNb_2O_8$ with the monoclinic structure. There were no significant changes and no peaks of chemical compositions of H_3BO_3 or B_2O_3 existed in all the XRD patterns, which indicated that liquid phase of H_3BO_3 was existed in the samples and nonreactive with $MnZrNb_2O_8$ matrix. Rietveld refinement was performed on all the samples sintered at 1250 °C to examine the variation in bond length of cation-oxygen bonds and nature of bonding. All the refinement parameters and bond length of cation-oxygen bonds were given in Table 1. It was found that the lattice parameters of the H_3BO_3-doped $MnZrNb_2O_8$ ceramics were approximately equal to the lattice parameters of pure phase $MnZrNb_2O_8$ ceramics, which also indicated that the H_3BO_3 didn't dissolve into the $MnZrNb_2O_8$ phase.

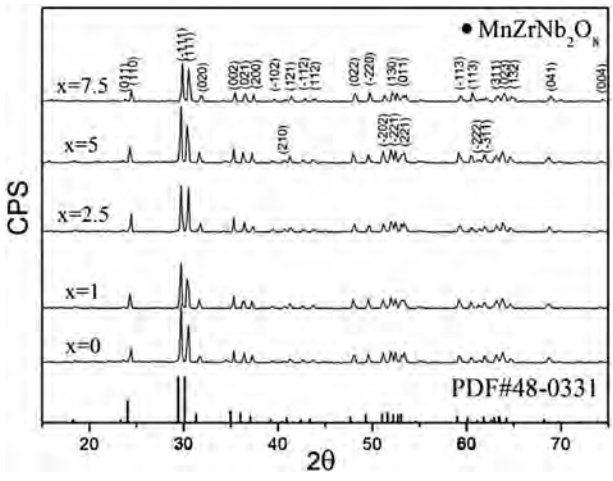

Fig. 1. XRD patterns of $MnZrNb_2O_8$ ceramics with different amounts of H_3BO_3 addition sintered at 1250 °C.

The SEM micrographs of $MnZrNb_2O_8$ + x wt% H_3BO_3 (x = 0, 1, 2.5, 5, 7.5) ceramics sintered at 1250 °C for 4 h were given in Fig. 2. As shown in Fig. 2(a), it was easily found that some pores were existed in pure-phase $MnZrNb_2O_8$ ceramic sintered at 1250 °C. Well-dense microstructures with grain sizes of 3–5 μm were observed in the sample when 1 and 2.5 wt% H_3BO_3 were added. As shown in Fig. 2(b-c), the porosity on the surface of sample significantly decreased, which was mainly due to the formation of liquid phase. During the sintering possess, the liquid phase covered the solid surfaces and worked as the liquid bridge between particles. In addition, the liquid phase decreased the friction among the $MnZrNb_2O_8$ particles and exerted a capillary force, which could rearrange the particles more easily and improve the density of the ceramics [17]. As the amount of H_3BO_3 was over 1 wt%, the apparent densities of $MnZrNb_2O_8$ ceramics slightly decreased and some pores were observed in Fig. 2(d-e), which were mainly due to the trapped porosity associated with grain growth and the formation of pores by the evaporation of excess glass components [18,19]. Thus, it was considered that a small amount of H_3BO_3 doping played an important role in reducing the sintering temperature due to the prominent effect of liquid-phase sintering mechanism.

Due to the H_3BO_3 addition, the theoretical density of $MnZrNb_2O_8$ ceramics couldn't be calculated accurately. Consequently, the apparent densities were used to characterize the sintering properties. The apparent densities of $MnZrNb_2O_8$ ceramics with H_3BO_3 addition from 0 to 7.5 wt% as a function of sintering temperatures were given in Fig. 3(a). As the sintering temperatures increasing from 1050 to 1250 °C, the apparent densities of the samples increased and the maximum apparent densities were obtained at 1250 °C. Fig. 3(b) illustrated the relationship between H_3BO_3 contents and apparent densities of the $MnZrNb_2O_8$ ceramics sintered at 1250 °C. It was reported in our previous work that the relative density of the pure phase $MnZrNb_2O_8$ ceramics was around 95% with the addition of 1 wt% H_3BO_3 at 1250 °C [14]. With the amounts of H_3BO_3 increasing to 1 wt%, the apparent densities significantly increased from 5.03 to 5.20 g/cm^3. Combining the above results shown in Fig. 2(b), it was demonstrated that the liquid phase at the grain boundary effectively eliminated the pores and increased the apparent density of the samples. For the 1 wt% H_3BO_3-added ceramics, the obtained apparent density of 5.20 g/cm^3 at 1250 °C was corresponded to that of the pure phase $MnZrNb_2O_8$ ceramics sintered at 1325 °C [14]. Thus, it was considered that the small amount of H_3BO_3 doping played an important role in decreasing the sintering temperature and improving the apparent densities. Thereafter, the apparent densities slightly decreased from 5.20 to 4.86 g/cm^3 as the contents of H_3BO_3 over 1 wt%. In general, the liquid phase accelerates the mass transportation and assists the densification of the ceramics. However, when sintering aids are excessive, the apparent densities are reduced by the addition of H_3BO_3, which is mainly due to the trapped porosity associated with grain growth and formation of pores by the evaporation of excess glass components. Thus, the density and microwave properties are degraded [20].

The dielectric constant of $MnZrNb_2O_8$ ceramics sintered at

Table 1
The crystal parameters, Nb-site bond length, bond valence parameters (R_{Nb-O}), bond valence (V_{Nb-O}), distortion of the oxygen octahedral and τ_f values of $MnZrNb_2O_8$ ceramics with different amounts of H_3BO_3 addition.

H_3BO_3 contents	0%	1%	2.5%	5%	7.5%
a (Å)	4.84878	4.87175	4.86456	4.84474	4.84965
b (Å)	5.66908	5.66497	5.67921	5.68847	5.69217
c (Å)	5.17735	5.17563	5.17031	5.17977	5.14517
β	91.6953	91.0754	91.0576	91.7172	91.5719
V (Å^3)	142.25	142.81	142.82	142.69	141.69
Nb–O(1)^1 × 2(Å)	1.7421	1.7479	1.7466	1.7428	1.7344
Nb–O(1)^2 × 2(Å)	2.0015	1.9982	2.0007	2.0063	2.0033
Nb–O(2) × 2(Å)	1.8968	1.9063	1.9066	1.8984	1.8980
R_{Nb-O} (Å)	1.911	1.911	1.911	1.911	1.911
V_{Nb-O}	6.8013	6.7136	6.7122	6.7622	6.8534
$\triangle_{Doctahedron}$ (%)	13.80	13.28	13.48	14.00	14.31
τ_f	−52.11	−8.44	−16.15	−9.19	−17.45

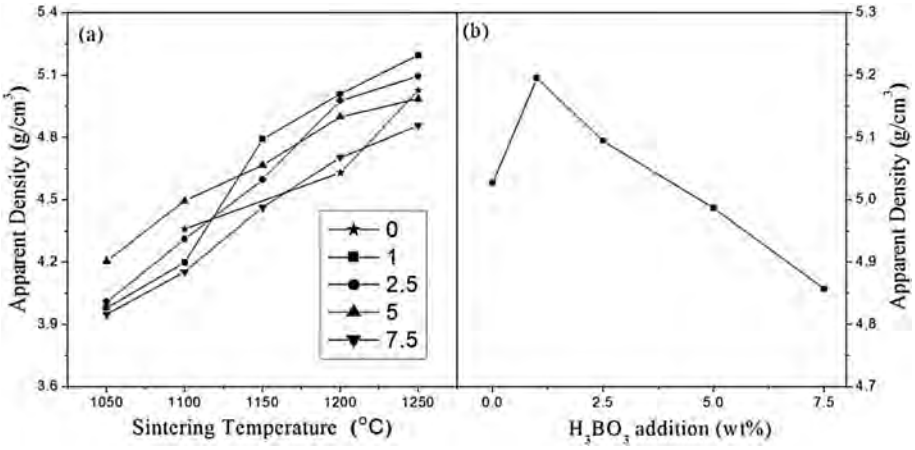

Fig. 2. SEM micrographs of $MnZrNb_2O_8$ ceramics with different amounts of H_3BO_3 addition sintered at 1250 °C (a–e corresponding to x = 0, x = 1, x = 2.5, x = 5 and x = 7.5 wt%).

different temperatures was illustrated in Fig. 4(a). In general, the dielectric constant of the microwave dielectric materials mainly depends on the density, secondary phase, dielectric polarizability and structure character [21,22]. As shown in Fig. 4(a), the ε_r values of all the samples increased with the sintering temperature increasing from 1050 to 1250 °C. Especially, the ε_r values of samples with 1 wt% H_3BO_3 steadily increased from 16.84 to 25.80 and saturated at ≈25 in the temperature region of 1200–1250 °C. The curve of ε_r values showed a similar tendency with those of apparent density shown in Fig. 3(a), which were sensitive to dense degree of ceramics significantly. The dielectric constants of the ceramics with different H_3BO_3 addition sintered at 1250 °C were illustrated in Fig. 4(b). As shown in Fig. 4(b), the ε_r values firstly increased from 24.62 to 25.80 with the H_3BO_3 addition increasing from 0 to 1 wt%. Thereafter, the ε_r values gradually decreased from 25.80 to 22.07 as the contents of H_3BO_3 over 1 wt%, which indicated that the apparent density was the most important extrinsic factor in controlling the dielectric constants in this work. Therefore, the best dielectric constant was observed for the best densification and the ε_r reached a maximum value of 25.80 when the H_3BO_3 content was 1 wt% at 1250 °C.

In general, several factors contribute to the dielectric loss in the range of microwave frequencies and these factors can be divided into two parts: the intrinsic loss and the extrinsic loss. Intrinsic losses are mainly caused by lattice vibration modes while extrinsic losses are dominated by second phases, oxygen vacancies, grain sizes and densification or porosity [21,22]. As shown in Fig. 5(a),(b), the $Q{\cdot}f$ values of all the samples gradually increased with the sintering temperature increasing from 1050 to 1250 °C and reached the maximum values at 1250 °C. The remarkable increase of $Q{\cdot}f$ values ranging from 1050 to 1250 °C was also related to the reduction of porosity according to the results of apparent densities shown in Fig. 3(a). Moreover, the 1 wt% H_3BO_3-doped $MnZrNb_2O_8$ ceramic exhibited the highest $Q{\cdot}f$ value of 28,419 GHz, which was attributed to the higher apparent density and the homogeneous microstructure. It was considered that any effort to improve densification would eventually lead to an increase in the $Q{\cdot}f$ values, since the volatile impurities and secondary phases associated with porosity eventually aggravate loss factor. However, the $Q{\cdot}f$ values slightly decreased with the increasing of H_3BO_3 over 1 wt%. Some investigations reported that the $Q{\cdot}f$ values were mainly affected by intrinsic factors when the prepared samples reached nearly full density [18,23], while the large dielectric loss of the liquid phase could also increase the dielectric loss of the ceramics. Thus, it was considered that the liquid phase can contribute to the grain growth while the low $Q{\cdot}f$ values of the liquid phase can decrease the $Q{\cdot}f$ values of the ceramics with the H_3BO_3 addition.

In general, the temperature coefficient of resonant frequency (τ_f) is related to temperature coefficient of dielectric constant (τ_ε) and the linear thermal expansion coefficient (α_L) as Eq. (2).

$$\tau_f = -\alpha_L - \frac{1}{2}\tau_\varepsilon \tag{2}$$

where the linear thermal expansion coefficient (α_L) is in the range of 10 ppm/°C for all the ceramics [24]. So τ_f mainly depends on temperature coefficient of dielectric constant (τ_ε). From the macroscopic Clausius-Mosotti equation, the temperature

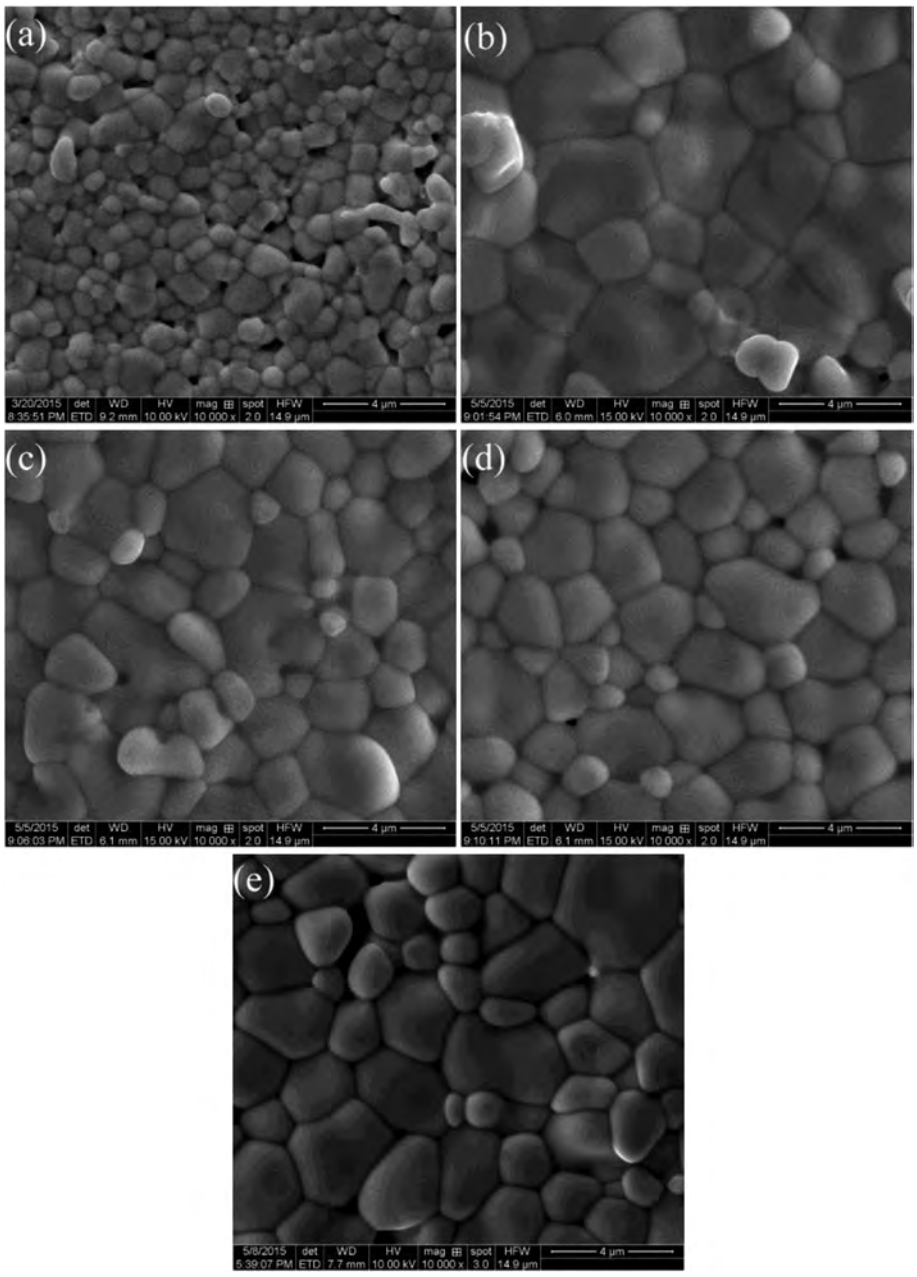

Fig. 3. (a) Apparent densities of $MnZrNb_2O_8$ ceramics as a function of H_3BO_3 content and sintering temperature. (b) Apparent densities of $MnZrNb_2O_8$ ceramics with different amounts of H_3BO_3 addition sintered at 1250 °C.

coefficient of dielectric constant can be derived as follows:

$$\tau_\varepsilon = \frac{1}{\varepsilon_r}\left(\frac{\partial \varepsilon_r}{\partial T}\right) = \frac{(\varepsilon_r - 1)(\varepsilon_r + 2)}{3\varepsilon_r} \times \left[\frac{1}{\alpha_m}\left(\frac{\partial \alpha_m}{\partial T}\right)_V + \frac{1}{\alpha_m}\left(\frac{\partial \alpha_m}{\partial V}\right)_T \left(\frac{\partial V}{\partial T}\right)_P - \frac{1}{V}\left(\frac{\partial V}{\partial T}\right)_P\right] \quad (3)$$

where α_m and V indicated the polarizability and volume of a small sphere, respectively. According to Bosman and Havinga [24], the second and third terms in the square brackets are related to the volume expansion, which have nearly equal magnitude and opposite sign. Therefore, the effect of these terms is negligible and the τ_ε is mainly dependent on the first part influenced by the crystal structure. Kim et al. reported that the distortion of the oxygen octahedral in [BO6] oxygen octahedral had a closely relation with τ_f. In addition, the bond valence between the octahedral-site cations and oxygen would affect the distortion of the oxygen octahedral. Thus the τ_f values would also decrease with the bond valence increasing [25,26]. In this work, the distortion of the oxygen octahedral was defined as [27]:

$$\Delta_{\text{octahedran}} = \frac{\text{B} - \text{O distance}_{\max} - \text{B} - \text{O distance}_{\min}}{\text{B} - \text{O distance}_{average}} \quad (4)$$

and the bond valence of all the [BO6] oxygen octahedral was calculated as follows [28]:

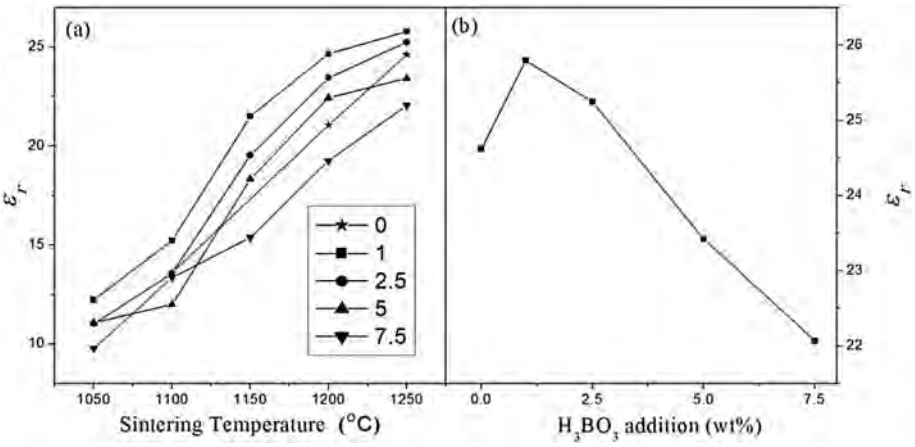

Fig. 4. (a) Dielectric constant of $MnZrNb_2O_8$ ceramics as a function of H_3BO_3 content and sintering temperature (b) Dielectric constant of $MnZrNb_2O_8$ ceramics with different amounts of H_3BO_3 addition sintered at 1250 °C.

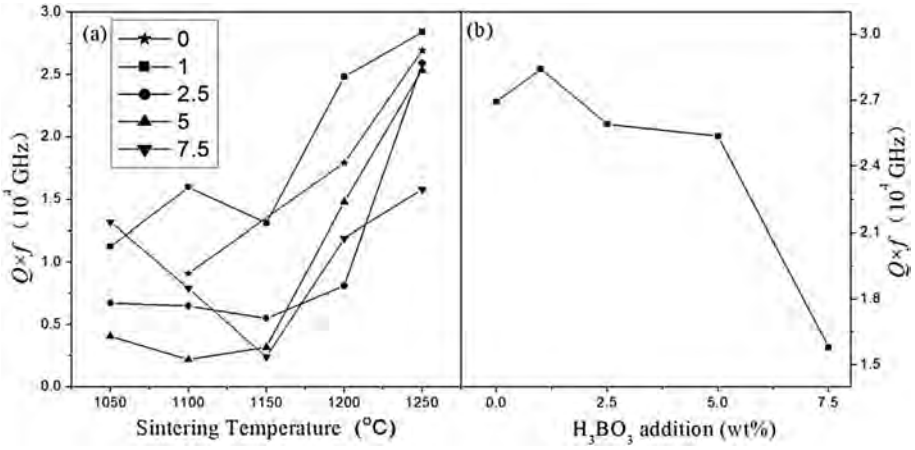

Fig. 5. (a) The *Q*·*f* values of $MnZrNb_2O_8$ ceramics as a function of H_3BO_3 content and sintering temperature (b) The *Q*·*f* values of $MnZrNb_2O_8$ ceramics with different amounts of H_3BO_3 addition sintered at 1250 °C.

$$V_{ij} = \sum v_{ij} \tag{5}$$

$$v_{ij} = \exp\left(\frac{R_{ij} - d_{ij}}{b'}\right) \tag{6}$$

where the V_{ij} represented the sum of all of valences from a given atom i, R_{ij} indicated the bond valence parameter, d_{ij} indicated the length of a bond between atoms i and j, and b' indicated a universal constant equal to 0.37. The Nb-site bond length, bond valence parameters ($R_{Nb\text{-}O}$), bond valence (V_{Nb-O}), distortion of the oxygen octahedral and τ_f values of $MnZrNb_2O_8$ ceramics with different amounts of H_3BO_3 addition were shown in Table 1. The correlation among distortion of the oxygen octahedral, bond valence of the [BO6] oxygen octahedral and τ_f values sintered at 1250 °C with different amount of H_3BO_3 were also shown in Fig. 6. As shown in Fig. 6, with the amounts of H_3BO_3 increasing from 0 to 1 wt%, the τ_f values of $MnZrNb_2O_8$ ceramics increased from −52.1 to −8.4 ppm/°C. Thereafter, the τ_f values fluctuated from −8.4 to −17.5 ppm/°C with the increasing of H_3BO_3 contents from 1 to 7.5 wt%. The distortion and bond valence of the oxygen octahedral showed an opposite trend that the values decreased first and then increased with H_3BO_3 contents increasing from 0 to 7.5 wt%. Although the mechanism of the τ_f values was unclear now, it could be reasonably

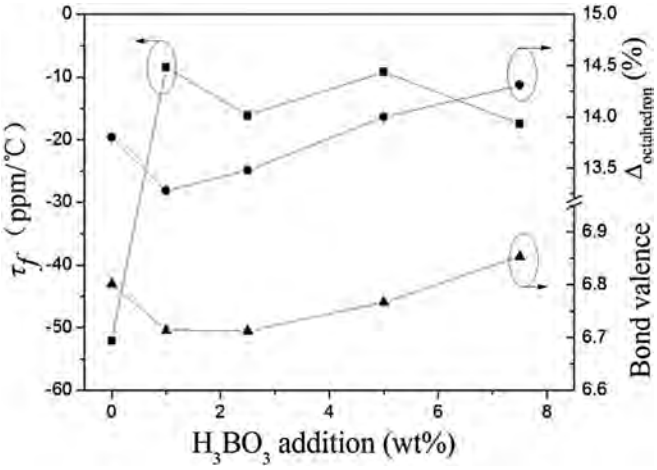

Fig. 6. The τ_f values, Nb-site bond valence and the distortion of the oxygen octahedral of the ceramics with different amount of H_3BO_3 sintered at 1250 °C for 4 h.

believed that the liquid phase should be responsible for the variation of the τ_f values and the addition of appropriate H_3BO_3 could adjust the τ_f values of $MnZrNb_2O_8$ ceramics to zero. Typically, 1 wt%

H_3BO_3-doped $MnZrNb_2O_8$ ceramics sintered at 1250 °C for 4 h exhibited promising microwave dielectric properties of $\varepsilon_r = 25.80$, $Q \cdot f = 28{,}419$ GHz and $\tau_f = -8.4$ ppm/°C, which were superior than the properties of the pure phase $MnZrNb_2O_8$ ceramics in our previous report [14].

4. Conclusions

The effects of H_3BO_3 addition on the sinterability and microwave dielectric properties of $MnZrNb_2O_8$ ceramics were investigated. Only a single phase $MnZrNb_2O_8$ was formed in the $MnZrNb_2O_8$ ceramics with H_3BO_3 addition at different sintering temperatures for 4 h. The liquid phase assisted the densification of the ceramics at lower sintering temperatures and the microwave dielectric properties were mainly depended on the apparent densities of the samples. In addition, the τ_f values were shifted to positive direction with the H_3BO_3 addition, which indicated that the appropriate H_3BO_3 addition could contribute to densification and the microwave dielectric properties of the ceramics. At 1250 °C, the $MnZrNb_2O_8$ ceramic with 1 wt% H_3BO_3 exhibited excellent properties: $\varepsilon_r = 25.80$, $Q \cdot f = 28{,}419$ GHz and $\tau_f = -8.4$ ppm/°C, which would make these ceramics promising for applications in microwave components.

Acknowledgments

This work was supported by the project development plan of Science and Technology of Jinan City (No.201303061), Jinan City Youth Science and Technology Star Project (No.2013035), the National Training Plan Innovation Project of college students (No.201510427001) and National Natural Science Foundation (No. 51472108).

References

[1] S. Nishigaki, H. Kato, S. Yano, R. Kamimure, Ceram. Am. Ceram. Soc. Bull. 66 (1987) 1405–1410.
[2] K. Wakino, K. Minai, H. Tamura, J. Am. Ceram. Soc. 67 (1984) 278–281.
[3] T. Takada, S.F. Wang, S. Yoshikawa, et al., J. Am. Ceram. Soc. 77 (1994) 1909–1916.
[4] H.T. Wu, L.P. Zhao, J. Univ. Jinan Sci. Tech. 30 (2016) 177–183.
[5] J.K. Plourde, D.F. Linn, H.M.J. O'Bryan, et al., J. Am. Ceram. Soc. 58 (1975) 418–420.
[6] P. Zhang, Z.K. Song, Y. Wang, et al., J. Alloys Compd. 581 (2013) 741–746.
[7] W. Wang, L.Y. Li, S.M. Xiu, et al., J. Alloys. Compd. 639 (2015) 359–364.
[8] Y.Z. Hao, H. Yang, G.H. Chen, et al., J. Alloys. Compd. 552 (2013) 173–179.
[9] T.W. Zhang, R.Z. Zuo, Cream. Int. 40 (2014) 15677–15684.
[10] H.T. Wu, Q.J. Mei, J. Alloys. Compd. 651 (2015) 393–398.
[11] H.T. Wu, J.D. Guo, J.X. Bi, et al., J. Alloys Compd. 661 (2016) 535–540.
[12] D. Ramarao, V.R.K. Murthy, Scr. Mater. 69 (2013) 274–277.
[13] A. Baumgarte, R. Blachnik, J. Alloys Compd. 215 (1994) 117–120.
[14] H.L. Pan, Z.B. Feng, J.X. Bi, et al., J. Alloys Compd. 651 (2015) 440–444.
[15] B.W. Hakki, P.D. Coleman, IEEE Trans. Microw. Theory Tech. 8 (1960) 402–410.
[16] W.E. Courtney, IEEE Trans. 18 (1970) 476–485.
[17] W.S. Kim, T.H. Kim, E.S. Kim, et al., Jpn. J. Appl. Phys. 37 (1998) 5367–5371.
[18] K.M. Manu, P.S. Anjana, M.T. Sebastian, Mater. Lett. 65 (2011) 565–567.
[19] P.V. Bijumon, M.T. Sebastian, Mater. Sci. Eng. B 123 (2005) 31–40.
[20] W.W. Cho, K.I. Kakimoto, H. Ohsato, Mat. Sci. Eng. B 121 (2005) 48–53.
[21] S.D. Ramarao, V.R.K. Murthy, Dalton Trans. 44 (2015) 2311–2324.
[22] L.X. Li, H. Sun, H.C. Cai, et al., J. Alloys Compd. 639 (2015) 516–519.
[23] C.L. Huang, M.H. Weng, Mater. Res. Bull. 35 (2000) 1881–1888.
[24] A.J. Bosman, E.E. Havinga, Phys. Rev. 129 (1963) 1593–1601.
[25] E.S. Kim, B.S. Chun, R. Freer, et al., J. Eur. Ceram. Soc. 30 (2010) 1731–1736.
[26] E.S. Kim, C.J. Jeon, J. Eur. Ceram. Soc. 30 (2010) 341–346.
[27] F. Lichtenberg, A. Herrnberger, K. Wiedenmann, J. Solid State Chem. 36 (2008) 253–387.
[28] P. Zhang, Y.G. Zhao, J. Liu, et al., J. Alloys Compd. 640 (2015) 90–94.